Impact of measurement uncertainties on universal scaling of MHD turbulence

G. Gogoberidze,[1,2]⋆ S. C. Chapman,[1] B. Hnat[1] and M. W. Dunlop[1,3,4,5]

[1]*Centre for Fusion, Space and Astrophysics, University of Warwick, Coventry CV4 7AL*
[2]*Institute of Theoretical Physics, Ilia State University, Cholokashvili Ave. 3/5, Tbilisi 0162, Georgia*
[3]*Rutherford-Appleton Laboratory, Chilton, Oxfordshire OX11 0QX*
[4]*CSSAR, CAS, PO Box 8701, Beijing 100190, China*
[5]*The Blackett Laboratory, Imperial College London, London SW7 2AZ*

ABSTRACT

Quantifying the scaling of fluctuations in the solar wind is central to testing predictions of turbulence theories. We study spectral features of Alfvénic turbulence in fast solar wind. We propose a general, instrument-independent method to estimate the uncertainty in velocity fluctuations obtained by in situ satellite observations in the solar wind. We show that when the measurement uncertainties of the velocity fluctuations are taken into account the less energetic Elsasser spectrum obeys a unique power law scaling throughout the inertial range as prevailing theories of magnetohydrodynamic (MHD) turbulence predict. Moreover, in the solar wind interval analysed, the two Elsasser spectra are observed to have the same scaling exponent $\gamma = -1.54$ throughout the inertial range.

Key words: turbulence – Solar wind.

1 INTRODUCTION

Universality in isotropic, homogeneous turbulence is expressed through its statistical scaling properties. In the absence of intermittency, the scaling exponent for the inertial interval of hydrodynamic turbulence is completely determined by the assumption of self-similarity (Kolmogorov 1941), leading to the well-known unique $-5/3$ power spectral exponent. This is not the case for magnetohydrodynamic (MHD) turbulence where the magnetic field introduces an additional physical quantity with the dimension of velocity, namely the Alfvén velocity (Chapman, Hnat & Kiyani 2008) and indeed it is an open question as to whether the scaling is universal. Detailed theoretical models of MHD turbulence are thus needed to predict the scaling exponent, and its precise observational determination is essential in order to validate these theories.

In situ satellite observations of the solar wind magnetic field and bulk flow span several decades in temporal scales and offer a 'natural laboratory' for the study of MHD turbulence; the Reynolds number exceeds $\sim 10^5$ (Matthaeus et al. 2005). They have been extensively used to test theoretical predictions of MHD turbulence (see, e.g., Marsch & Tu 1990; Bruno & Bavassano 1991; Grappin, Velli & Mangeney 1991; Podesta et al. 2009; Podesta & Borovsky 2010; Wicks et al. 2010; Chen et al. 2011 and references therein). The Elsasser fields, $\mathbf{Z}^\pm = \mathbf{v} \pm \mathbf{B}/\sqrt{4\pi\rho}$, where $\mathbf{v}$ and $\mathbf{B}$ are the velocity and magnetic fields, respectively, and ρ is the average density,

represent eigenfunctions of counter propagating (with respect to the mean magnetic field) Alfvén waves and therefore they are primary fields for the study of incompressible MHD turbulence. Fluctuations in the fast solar wind are strongly imbalanced – there is more power in Alfvén waves propagating outward from the sun than towards it (e.g. Bruno & Carbone 2005) so that the power in $\mathbf{Z}^+$ typically dominates over that in $\mathbf{Z}^-$. As with many other quantities that characterize physical properties of the turbulent flow [e.g. Yaglom relations (Politano & Pouquet 1998; Carbone et al. 2009; Smith et al. 2009) and dynamic alignment angle (Podesta et al. 2009)], the Elsasser variables combine velocity and magnetic field fluctuations as a function of temporal scale. Pioneering observations from the *Helios* missions showed that in the fast solar wind streams at 0.3 au the observed power spectrum of $\mathbf{Z}^-$ (the sub-dominant component) did not follow a single power law shape. At very low frequencies corresponding to '1/f' range ($f < 3 \times 10^{-4}$ Hz), the spectral slope γ_- was close to Kolmogorov's value ($\gamma_- \approx -1.67$), whereas in the low frequency part of the inertial interval ($5 \times 10^{-4} < f < 2 \times 10^{-3}$Hz) the $\mathbf{Z}^-$ power spectrum was much shallower, with $\gamma_- \approx -1.3 - 1.4$ (Grappin, Mangeney & Marsch 1990; Marsch & Tu 1990; Bruno & Bavassano 1991; Grappin et al. 1991). At 1 au, the observed spectral slope was approximately equal to Kolmogorov's value both in the 1/f range and low frequency part of the inertial interval (Marsch & Tu 1990). Recently using high cadence *WIND* observations, Wicks et al. (2010) studied spectral features of the Elsasser variables in the high frequency part of the inertial interval for the first time. They showed that at 1 au (in accordance with earlier studies) in the low frequency part of

⋆E-mail: grigol_gogoberidze@iliauni.edu.ge

the inertial interval ($10^{-3} < f < 10^{-2}$ Hz) $\mathbf{Z}^-$ nearly follows Kolmogorov scaling which at higher frequencies ($f > 10^{-2}$ Hz) is more shallow with $\gamma_- \approx -1.3$. The absence of single scaling of the sub-dominant Elsasser field in the entire inertial interval contradicts all recently developed models of strong, anisotropic imbalanced MHD turbulence (Lithwick, Goldreich & Sridhar 2007; Beresnyak & Lazarian 2008; Chandran 2008; Perez & Boldyrev 2009; Podesta & Bhattacharjee 2010) which predict a single scaling for sub-dominant $\mathbf{Z}^-$ spectrum (this does not mean that the spectral indices of the dominant and sub-dominant Elsasser fields should be the same in the inertial interval). They are also inconsistent with the results of recent high resolution direct numerical simulations of imbalanced MHD turbulence which showed single scaling of the sub-dominant Elsasser field in the inertial interval (Beresnyak & Lazarian 2008; Perez & Boldyrev 2009, 2010).

Control of observational uncertainty in the in situ observations is non-trivial, although these errors often have known bounds. There are different challenges for magnetic field and velocity measurements; solar wind velocity observations are intrinsically more uncertain compared to the magnetic field data. In this paper, we propose a general, instrument-independent method to estimate the uncertainty on velocity field fluctuations direct from the data. We obtain the systematic shift that this uncertainty introduces into observed spectral exponents. We will see that the shallower $\mathbf{Z}^-$ spectrum at high frequencies can be entirely accounted for by this uncertainty in the velocity data and the observations of the $\mathbf{Z}^{\pm}$ spectra may in fact within achievable accuracy of the observations be in agreement with the predictions of theory and numerical simulations.

2 DATA ANALYSIS

We use data obtained by the *WIND* spacecraft at 3 s resolution. Magnetic field data are provided by the Magnetic Field Investigation (MFI) instrument (Lepping et al. 1995) and density and velocity data by the three dimensional plasma (3DP) instrument (Lin et al. 1995). We use observations made during a quiet fast stream. The start time of the interval is 06:00 of 2008 April 06 and the stop time is 12:00 of 2008 April 08. During this interval, the solar wind speed remained above 550 km s^{-1}. The energy of compressive fluctuations was an order of magnitude lower than that of incompressible fluctuations and, consequently, magnetic and velocity fluctuations, being mainly Alfvénic, were dominated by the components perpendicular to the local mean field. The mean field, $\bar{\mathbf{B}}(t, \tau)$, at some time t and on scale τ is defined as the magnetic field averaged over the interval $[t - \tau, t + 2\tau]$. The fluctuations of the velocity and magnetic field are defined by standard expressions $\delta\mathbf{v}(t, \tau) = \mathbf{v}(t + \tau) - \mathbf{v}(t)$ and $\delta\mathbf{B}(t, \tau) = \mathbf{B}(t + \tau) - \mathbf{B}(t)$, respectively.

There are several sources of uncertainty in the solar wind velocity measurements (Podesta & Borovsky 2010). The first source is the uncertainty in assessment of the proton distribution function. In addition, in common with all velocity in situ observations, the 3 s velocity observations on *WIND* (as well as any other in situ measurements of moments of the particle distribution function) are quantized before ground transmission and this quantization results in high frequency noise or quantization noise. These, and other contributions to observational uncertainty, decorrelate the velocity and magnetic field fluctuations at high frequencies. White, delta correlated noise provides a reasonable generic, instrument-independent model for the uncertainty (Podesta & Borovsky 2010). Any measurement of a velocity component fluctuation δv_o can then be represented as a sum of the 'real' turbulent signal δv_s and noise δv_n which has zero mean and standard deviation ε, so $\delta v_o = \delta v_s + \delta v_n$.
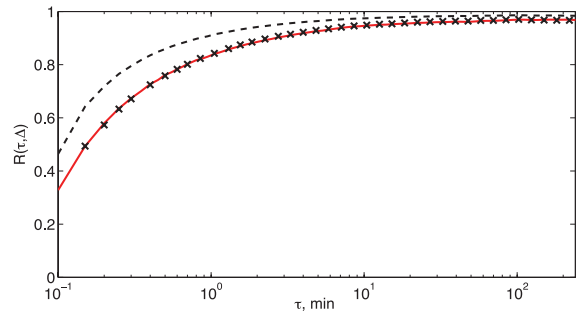

Figure 1. Autocorrelation functions $R_{\delta B_y}(\tau, \Delta)$ (black dashed line) of the GSE y component of the magnetic field fluctuation and $R_{\delta v_y}(\tau, \Delta)$ (red solid line) with the time lag $\Delta = 3$ s.

Note that the rms value of a single velocity measurement v_n used to characterize velocity uncertainties in other studies (Podesta et al. 2009; Podesta & Borovsky 2010) is, in our notations, $\varepsilon/\sqrt{2}$. In what follows, we will neglect the uncertainties in the magnetic field measurements since generally these are small relative to those of the velocity measurements (Podesta & Borovsky 2010; Wicks et al. 2010).

We will first quantify the velocity uncertainty from the data. We will exploit the fact that both the turbulent signal and the noise are random variables with distinct characteristic autocorrelation time-scales. We make a key assumption that the autocorrelation time-scale of the underlying turbulent signal is that observed in the magnetic field component fluctuations δB_o (they have negligible noise) and that this is also the autocorrelation time-scale of the 'true' turbulent velocity component fluctuations δv_s. Any difference in the autocorrelation functions of the observed δv_o and δB_o are thus attributable to the (delta-correlated) noise δv_n on the velocity. The autocorrelation coefficient (AC) of a component δv on time lag Δ is $R_{\delta v}(\tau, \Delta) \equiv \langle \delta v(t + \Delta, \tau)\delta v(t, \tau)\rangle/\langle \delta v(t, \tau)^2\rangle$, where angular brackets denote time averages with respect to the entire studied interval (i.e. with respect to all possible values of t). The ACs $R_{\delta B_o}(\tau, \Delta)$ and $R_{\delta v_o}(\tau, \Delta)$ for GSE y components of the magnetic field and velocity fluctuations are plotted in Fig. 1 for lag $\Delta = 3$s as a function of scale τ with black solid and red dashed lines, respectively. We see that the AC grows with scale τ for both signals and that the velocity AC is systematically lower than that of the magnetic field, consistent with the assumption of uncorrelated noise that principally affects the velocity signal. Given these assumptions one can construct a modelled noisy signal by adding uncorrelated noise to the magnetic field observations. The modelled noisy fluctuations $\delta B_{o+n} = \delta B_o + \delta B_n$, where δB_n are delta correlated Gaussian distributed random numbers with zero mean and standard deviation ε_B. The magnitude of the modelled noise ε_B can then be systematically varied. We first verify that this simple noise model is sufficient to reproduce the AC as a function of τ for the velocity fluctuations. The AC of the modelled δB_{o+n} is shown by the black crosses in Fig. 1 and this can be seen to closely coincide with the observed AC of velocity fluctuations δv_o. Assuming Alfvénic fluctuations the magnitude of ε_B used to generate this curve corresponds to an uncertainty in the velocity fluctuations of

$$\varepsilon_v \equiv \varepsilon_B \sqrt{\frac{\langle \delta v_o^2 \rangle}{\langle \delta B_{o+n}^2 \rangle}} = 4\,\text{km s}^{-1}. \tag{1}$$

Hereafter in this paper ε denotes the rms value of the observed velocity fluctuation δv, whereas ε_v denotes its estimate, derived using different methods described in the paper. Thus, $\varepsilon \sim 4$ km s^{-1} (which
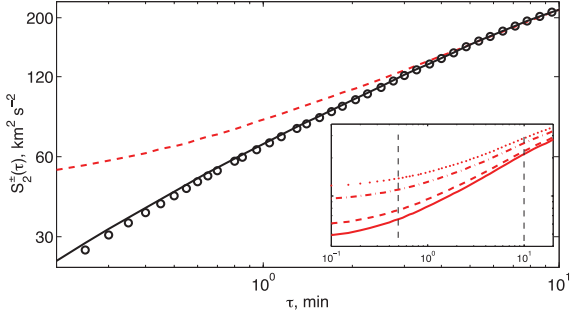
Figure 2. The normalized second-order structure functions: of the GSE z component of the sub-dominant Elsasser variable Z_z^- (red dashed line), of the dominant Elsasser variable Z_z^+ (black solid line) and S_2^- (circles, see the text for details). In the inset: the second-order structure functions of the sub-dominant Elsasser variable for different values of added Gaussian noise. Raw observations are denoted by the solid line, and added noise is equivalent to $\varepsilon_v = 2\,\mathrm{km\,s^{-1}}$ (dashed line), $\varepsilon_v = 4\,\mathrm{km\,s^{-1}}$ (dash-dotted line) and $\varepsilon_v = 5\,\mathrm{km\,s^{-1}}$ (dotted line).

corresponds to the uncertainty of a single velocity component of $\varepsilon/\sqrt{2} \sim 2.83\,\mathrm{km\,s^{-1}}$) is a reasonable estimate of the amplitude of the noise on the turbulent velocity signal. We will develop this idea to obtain a general method to estimate the uncertainty direct from the data. In the following section, we will compare our assessment of the velocity measurement uncertainties with the estimate derived in other studies. First, we will see how these uncertainties can affect measurements of scaling exponents and the conclusions that can be drawn from them.

In Fig. 2 we plot the observed second-order structure functions S_2 of a component of the fluctuations in the Elsasser variables, where the Elsasser components are given by $\delta Z_i^\pm(\tau) = \delta v_i(t, \tau) \pm \delta B_i(t, \tau)/\sqrt{4\pi\bar{\rho}}$ and $\bar{\rho}(\tau)$ is the local mean value of the density averaged over the time-scale of the fluctuations τ, i.e. over the interval $[t, t + \tau]$ and $S_2^\pm = \langle \delta Z_i^\pm(\tau)^2 \rangle$. The solid lines are the structure functions of GSE z components of the dominant δZ_z^+ (black solid line) and sub-dominant δZ_z^- (red dashed line) fields. They are normalized to have the same values at $\tau = 10\,\mathrm{min}$ scale on this plot; the power in δZ_z^+ is 20 times that in δZ_z^- at $\tau = 10\,\mathrm{min}$ scale. For the ideal statistical scaling of fully developed MHD turbulence, we anticipate the scaling $S_2 \sim \tau^{\zeta^\pm(2)}$ and turbulence theories predict constant values of $\zeta^\pm(2)$ over the entire inertial interval (they are directly related to the power spectral exponents $\gamma_\pm$ via $\gamma_\pm = -\zeta_\pm(2) - 1$). We can see that consistent with earlier studies (e.g. Wicks et al. 2010), the sub-dominant Elsasser variable does not follow a single power law in the inertial interval. A linear mean least-squares fit on the log–log plot over scales $30\,\mathrm{s} < \tau < 10\,\mathrm{min}$ gives $\gamma_+ = -1.54 \pm 0.02$ and $\gamma_- = -1.40 \pm 0.02$, consistent with previous observations (Marsch & Tu 1990; Bruno & Bavassano 1991; Grappin et al. 1991; Wicks et al. 2010).

A quantitative demonstration of the effect of noise is provided by calculating $S_2^-(\delta B_{o+n}, \delta v_o) \equiv \langle [\delta v_{i,o} - (\delta B_{i,o} + \delta B_{i,n})/\sqrt{4\pi\bar{\rho}}]^2 \rangle$ which for uncorrelated noise is equivalent to $S_2^-(\delta B_o, \delta v_o) + \varepsilon_v^2$. Here a different 'Alfvénic' relation, $\varepsilon_v = \varepsilon_B/\sqrt{4\pi\bar{\rho}}$, is used to relate the velocity and magnetic field uncertainties. This is shown in the inset of Fig. 2 for a range of amplitudes of δB_n, which are equivalent to velocity noise uncertainties of $\varepsilon_v = 2, 4$ and $5\,\mathrm{km\,s^{-1}}$. We can see that addition of 'white' (delta-correlated) noise always systematically 'flattens' these curves, that is, it decreases the value of the scaling exponent; for $\varepsilon_v = 4\,\mathrm{km\,s^{-1}}$ the pseudo-noise strongly

affects S_2^- at all scales in the inertial interval. The 'flattening' of the pseudo-noisy $S_2^-(\delta B_{o+n}, \delta v_o)$ curve, that is, the change in the mean exponent over time-scales $30\,\mathrm{s} < \tau < 10\,\mathrm{min}$ is $\Delta\gamma_- \approx 0.13$, is close to the observed difference between exponents of the dominant and sub-dominant fields ($\gamma_- - \gamma_+ = 0.14$); hence, this difference could be just due to noise in the velocity data.

We now obtain an estimate of the structure function in the absence of the noise in the velocity, $S_2^-(\delta B_o, \delta v_s) \equiv \langle (\delta Z_s^-)^2 \rangle$, where $\delta Z_s^- = \delta v_s - \delta B_o/\sqrt{4\pi\bar{\rho}}$. We have that the observed structure function $S_2^-(\delta B_o, \delta v_o) = \langle (\delta Z_s^- + \delta v_n)^2 \rangle = S_2^-(\delta B_o, \delta v_s) + 2\langle \delta Z_s^- \delta v_n \rangle + \varepsilon^2$. Assuming as before that the turbulent signal and the velocity error are uncorrelated ($\langle \delta Z_s^- \delta v_n \rangle = 0$), we obtain $S_2^-(\delta B_o, \delta v_s) = S_2^-(\delta B_o, \delta v_o) - \varepsilon^2$. The plot of our estimated $S_2^-(\delta B_o, \delta v_s)$ is given by black circles in Fig. 2 for $\varepsilon = 4\,\mathrm{km\,s^{-1}}$. This error-compensated sub-dominant $S_2^-(\delta B_o, \delta v_s)$ curve now has a single scaling throughout the inertial range, consistent with current theories and numerical predictions (Lithwick et al. 2007; Beresnyak & Lazarian 2008; Chandran 2008; Perez & Boldyrev 2009; Podesta & Bhattacharjee 2010; Podesta 2011a,b). We can also see that the slope of $S_2^-(\delta B_o, \delta v_s)$ coincides quite closely with the observed slope of the dominant Elsasser variable S_2^+. The uncertainty in the velocity that we have estimated from the data is thus sufficient to account for the departure in scaling between the $\delta \mathbf{Z}^-$ and $\delta \mathbf{Z}^+$ Elsasser variables and these observations may in fact within the achievable accuracy be in agreement with theories (Lithwick et al. 2007; Perez & Boldyrev 2009; Podesta & Bhattacharjee 2010) that predict a *single scaling* for $\delta \mathbf{Z}^-$ and $\delta \mathbf{Z}^+$.

We have verified that $\delta \mathbf{Z}^+$ is not strongly affected by velocity uncertainties of this amplitude: S_2^+ remains almost unchanged for $\varepsilon_v < 5\,\mathrm{km\,s^{-1}}$. This conclusion is also supported by the fact that as shown in Fig. 2, S_2^+ has a convex shape, which is typical for finite range hydrodynamic and MHD turbulence (Benzi et al. 1993; Chapman & Nicol 2009), whereas S_2^- is concave, consistent with 'shallowing' at small scales due to noise effects. In addition to the velocity measurement uncertainties, the Elsasser fields are also affected by uncertainties related to the density measurement. Our analysis shows that adding the same amount of relative modelled noise to the density data has negligible influence on the results. This is not surprising, as the definition of the Elsasser fields is in terms at the mean value of the density over scales, and this reduces the influence of density uncertainties due to the central limit theorem.

We now outline a method to explicitly determine the uncertainty as a function of scale τ and time lag Δ from the observations. We will generalize the approach shown in Fig. 1. Given the assumption that $R_{\delta B_o}(\tau, \Delta) = R_{\delta v_s}(\tau, \Delta)$ and again that the noise is delta correlated $\langle \delta v_n(t + \Delta) \delta v_n(t) \rangle = 0$, we can obtain the uncertainty from the AC directly:

$$\varepsilon = \langle \delta v_o(\tau)^2 \rangle \sqrt{1 - \frac{R_{\delta v_o}(\tau, \Delta)}{R_{\delta B_o}(\tau, \Delta)}}. \qquad (2)$$

The dependence of ε on scale τ derived by equation (2) for $\Delta = 3\,\mathrm{s}$ is presented in Fig. 3. The results obtained by applying equation (2) to x, y and z components of magnetic field and velocity fluctuations are given by solid, dotted and dash–dotted lines, respectively. The inset shows the dependence of ε on time lag Δ for $\tau = 1\,\mathrm{min}$. As we see, the results are consistent with the estimate of $\varepsilon = 4\,\mathrm{km\,s^{-1}}$ used above. Moreover, it can be seen that ε has very weak dependence on both τ and Δ, supporting a posteriori the assumption that uncorrelated white noise is a suitable approximation for the velocity uncertainty.

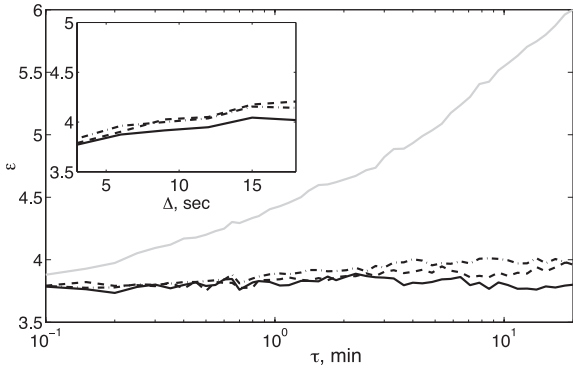**Figure 3.** The observational uncertainty ε derived by equation (2) for x (solid line), y (dashed) and z (dash–dotted) components of the perturbations for $\Delta = 3$ s. In the inset: Δ dependence of ε for $\tau = 1$ min. The grey line denotes the rms value of δv_p.

3 DISCUSSION

Recently, in situ solar wind data have been used by Podesta et al. (2009) to test the prediction of scale-dependent dynamic alignment in MHD turbulence (Boldyrev 2006). This relies on the determination of the angle between magnetic and velocity fluctuations perpendicular to the local mean magnetic field direction. The observational uncertainty is known to make a significant contribution to the component of the velocity perturbation perpendicular to the magnetic field perturbation $\delta v_p(t, \tau) = \delta \boldsymbol{B}_\perp \times \delta \boldsymbol{v}_\perp / \delta B_\perp$ even at quite large scales $\tau \sim 10$ min (Podesta et al. 2009). We plot the rms value of the observed $\delta v_{p,o}$ on Fig. 3 (grey line). As can be seen for fluctuations on scales τ of a few minutes or less, the observed $\delta v_{p,o}$ is almost entirely dominated by observational uncertainty. The estimate of the observational uncertainty in Podesta et al. (2009) gave a somewhat lower value, which in our notation is $\varepsilon \approx 1.5\sqrt{2}$ km s^{-1}. In Podesta et al. (2009), the alignment angle $\theta_A \equiv \arcsin(\langle \delta v_p \delta B_\perp \rangle / \langle \delta v_\perp \delta B_\perp \rangle) \approx \delta v_p / \sqrt{\langle \delta v_\perp(\tau)^2 \rangle}$ was used to estimate the observational uncertainty. In fact, correlation between $\delta B_\perp$ and $\delta v_\perp$ is much stronger than correlation between $\delta B_\perp$ and δv_p (because the latter at small scales is strongly dominated by the error). Detailed analysis shows that this increases the estimates in Podesta et al. (2009) by a factor ~ 1.6. Also, the local alignment angle between velocity and magnetic fields θ is a random variable with zero mean. Any measure of the alignment angle (such as the mean of the absolute value of the alignment angle) should thus be related to the standard deviation σ_θ of the angle. If for highly aligned cases we assume that θ is close to Gaussian distributed, then its absolute value is described by the half-normal distribution and its mathematical expectation is given by $\sigma_\theta \sqrt{1 - 2/\pi}$ (and not σ_θ) and this yields another factor of 1.2533 compared to the estimate of Podesta et al. (2009).

This uncertainty of ≈ 4 km s^{-1} in the velocity fluctuations will systematically reduce the scaling exponent of the velocity compared to that of the magnetic field, if as we have assumed here the uncertainty in the magnetic field can be neglected in such a comparison. We estimate that this uncertainty alone would result in a difference in the power spectral exponents of $\gamma_v - \gamma_B \approx 0.04$. This is less than the observed difference which is typically in the range ~ 0.1 (Perez & Boldyrev 2009) to ~ 0.2 (Tessein et al. 2009). These estimates are sufficiently close however to merit more detailed analysis.

Recently several attempts have been made to determine MHD energy cascade rates in the solar wind via Yaglom relations (Carbone et al. 2009; Smith et al. 2009), which relate third-order mixed mo-

ments of Elsasser variables with energy dissipation rates (Politano & Pouquet 1998)

$$\left\langle \delta Z_L^\mp |\delta Z^\pm|^2 \right\rangle = -\frac{4}{3} \epsilon^\pm r. \tag{3}$$

Here $\delta Z_L^\mp = \delta \boldsymbol{Z}^\mp \cdot \hat{\boldsymbol{r}}$ and $\epsilon^\pm$ are energy dissipation rates. Assuming as before that the turbulent signal and the velocity error are uncorrelated, and substituting $\delta v = \delta v_s + \delta v_n$, it is straightforward to show that velocity uncertainties have no influence on the third-order moments. This finding shows an important advantage of third-order moment analysis compared to the second-order structure function analysis which, as shown above, are significantly affected by the velocity uncertainties.

Finally, we have also applied the above methods to *WIND* observations of slow solar wind streams (with the wind speed below 400 km s^{-1}) during solar maximum and we found a significantly smaller value for the velocity uncertainty $\varepsilon \approx 2$ km s^{-1}. This difference may be a consequence of different plasma density in fast and slow solar wind streams. Alternatively, it is possible that the observed difference indicates the fact that the uncertainty of the velocity is strongly correlated with the solar wind speed. Detailed analysis of this topic will be presented elsewhere.

4 CONCLUSIONS

In summary, we have presented a general, instrument-independent method to determine uncertainty in the velocity fluctuations in single point measurements. We have shown that this uncertainty is sufficient to account for both the absence of single scaling of the sub-dominant Elsasser field and the difference of $\boldsymbol{Z}^\pm$ slopes in the inertial interval. Thus, our findings are able to report for the first time that the observations are, within the achievable accuracy, in agreement with the predictions of theory and numerical simulations.

REFERENCES

Benzi R., Ciliberto S., Tripiccione R., Baudet C., Massaioli F., Succi S., 1993, Phys. Rev. E, 48, R29
Beresnyak A., Lazarian A., 2008, ApJ, 682, 1070
Boldyrev S., 2006, Phys. Rev. Lett., 96, 115002
Bruno R., Bavassano B., 1991, J. Geophys. Res., 5, 7841
Bruno R., Carbone V., 2005, Living Rev. Sol. Phys. 2, 4
Carbone V., Marino R., Sorriso-Valvo L., Noullez A., Bruno R., 2009, Phys. Rev. Lett., 103, 061102
Chandran B. D. G., 2008, ApJ, 685, 646
Chapman S. C., Nicol R. M., 2009, Phys. Rev. Lett., 103, 241101
Chapman S. C., Hnat B., Kiyani K., 2008, Nonlinear Process Geophys., 15, 445
Chen C. H. K., Mallet A., Yousef T. A., Schekochihin A. A., Horbury T. S., 2011, MNRAS, 415, 3219
Grappin R., Mangeney A., Marsch E., 1990, J. Geophys. Res., 95, 8197
Grappin R., Velli M., Mangeney A., 1991, Ann. Geophys., 9, 416
Kolmogorov A. N., 1941, Dokl. Akad. Nauk SSSR 31, 538
Lepping R. P. et al., 1995, Space Sci. Rev., 71, 125
Lin R. P. et al., 1995, Space Sci. Rev., 71, 207
Lithwick Y., Goldreich P., Sridhar S., 2007, ApJ, 655, 269
Marsch E., Tu C.-Y., 1990, J. Geophys. Res., 95, 8211

Matthaeus W. H., Dasso S., Weygand J. M., Milano L. J., Smith C. W., Kivelson M. G., 2005, Phys. Rev. Lett., 95, 231101

Perez J. C., Boldyrev S., 2009, Phys. Rev. Lett., 102, 025003

Perez J. C., Boldyrev S., 2010, Phys. Plasmas, 17, 055903

Podesta J., 2011a, Phys. Plasmas, 18, 012906

Podesta J., 2011b, Phys. Plasmas, 18, 012907

Podesta J., Bhattacharjee A., 2010, ApJ, 718, 1151

Podesta J. J., Borovsky J. E., 2010, Phys. Plasmas, 17, 112905

Podesta J. J., Chandran B. D. G., Bhattacharjee A., Roberts D. A., Goldstein M. L., 2009, J. Geophys. Res., 114, 01107

Politano H., Pouquet A., 1998, Geophys. Res. Lett., 25, 273

Smith C. W., Stawarz J. E., Vasquez B. J., Forman M. A., MacBride B. T., 2009, Phys. Rev. Lett., 103, 201101

Tessein J. A., Smith C. W., MacBride B. T., Matthaeus W. H., Forman M. A., Borovsky J. E., 2009, ApJ, 692, 684

Wicks R. T., Horbury T. S., Chen C. H. K., Schekochihin A. A., 2010, MNRAS, 407, L31

This paper has been typeset from a TeX/LaTeX file prepared by the author.